

# Journal of Materials Chemistry B

Accepted Manuscript



This is an *Accepted Manuscript*, which has been through the Royal Society of Chemistry peer review process and has been accepted for publication.

*Accepted Manuscripts* are published online shortly after acceptance, before technical editing, formatting and proof reading. Using this free service, authors can make their results available to the community, in citable form, before we publish the edited article. We will replace this *Accepted Manuscript* with the edited and formatted *Advance Article* as soon as it is available.

You can find more information about *Accepted Manuscripts* in the [Information for Authors](#).

Please note that technical editing may introduce minor changes to the text and/or graphics, which may alter content. The journal's standard [Terms & Conditions](#) and the [Ethical guidelines](#) still apply. In no event shall the Royal Society of Chemistry be held responsible for any errors or omissions in this *Accepted Manuscript* or any consequences arising from the use of any information it contains.

## Graphene quantum dots conjugated albumin nanoparticles for targeted drug delivery and imaging of pancreatic cancer

Preeti Nigam<sup>a,\*,#</sup>, Shobha Waghmode<sup>b,#</sup>, Michelle Louis<sup>c</sup>, Shishanka Wangnoo<sup>c</sup>, Pooja Chavan<sup>b</sup>, Dhiman Sarkar<sup>a</sup>

Pancreatic cancer is considered to be the deadliest of all cancers due to its poor prognosis and resistance to conventional therapies. In this study the potential of hyaluronic acid functionalized and green fluorescent graphene quantum dots (GQDs) labeled human serum albumin nanoparticles for pancreatic cancer specific drug delivery and bioimaging was explored. GQDs with their tunable fluorescence properties and biocompatibility have attracted a lot of interest in recent years as compared to their metal semiconductor counterparts. We adopted lawsone (2-hydroxy 1,4 naphthoquinone) as a novel, reducing agent for synthesis of quantum dots and apart from excellent fluorescence of synthesized GQDs, a good quantum yield of ~14% was also obtained. Gemcitabine, the most preferred drug for pancreatic cancer treatment was encapsulated in albumin nanoparticles and it was observed that our nanoformulation significantly enhanced the bioavailability and sustained release property of the drug to pancreatic cancer cells *in-vitro*. Meanwhile GQDs mediated excellent bioimaging enhanced the efficacy of our system as drug delivery vehicle.

Pancreatic cancer originates from altered cells in pancreatic tissues. Adenocarcinoma which arises within the exocrine component of the pancreas is the most common type of pancreatic cancer. It possesses the worst mortality rate in all cancers and is the fourth most common cause of cancer-related deaths in the United States and the eighth worldwide due to its extremely poor prognosis in locally advanced or metastasized stage.<sup>1, 2</sup> Moreover pancreatic cancer is resistant to most of the conventional therapies that exhibit only palliative effect with minimal impact on survival. Due to the enriched tumor stromal component and disorganized vasculature of pancreatic cancer tissues, efficient delivery of therapeutic agents is quite difficult<sup>3-5</sup> thus it is imperative to discover innovative strategies for targeted drug delivery to treat this lethal disease.

In recent decades nanotechnology has shown great potential in the field of medicine with vast applications in diagnostic and therapeutic agents for cancer targeting and imaging.<sup>6-8</sup> It is a well known fact that chemotherapy exhibits massive side effects due to indiscriminate distribution of anticancer drug to cancerous and healthy cells. To minimize this, researchers from all over the world are contributing to develop nano-devices for cancer detection and delivering antineoplastic drugs to the cancer cells. Recently Food and Drug Administration approval of albumin-taxol nanoformulation (Abraxane-ABI 007), for the treatment of breast cancer, has boosted the research for the development of nanoparticle based targeted drug delivery systems.

The present study demonstrates a novel nanoformulation containing GQDs conjugated gemcitabine loaded human serum albumin (HSA) nanoparticles based targeted delivery and imaging system for pancreatic cancer. Albumin is the most abundant protein in our body and nanoformulations based on albumin are free from immunogenic and hemolytic problems. Moreover it is a well known fact that HSA can infiltrate tumor cells via gp60 pathway<sup>9</sup> that makes it an excellent drug delivery vehicle. Gemcitabine (Gem) is the most preferred drug for the treatment of pancreatic cancer but unfortunately it exhibits trivial impact on lifespan due to its inadequate cellular uptake and small half life.<sup>10, 11</sup> To overcome this dilemma, generally high and frequent doses of Gem are to be administered to the patient that often translates into systemic toxicity and resistance towards the drug hence outshining the drug's persuasive pharmacological effects. Hong et al. discovered that CD-44 positive cells are responsible for gemcitabine resistance in pancreatic cancer cells. CD-44 is a pancreatic cancer stem cell surface marker which is highly expressed on human pancreatic adenocarcinoma cells and is responsible for proliferation and reconstitution of resistant pancreatic cancer cells.<sup>11</sup> As a remedial application, targeted therapy against CD-44 cells can conquer drug resistance in the treatment of pancreatic cancer. Hyaluronic acid (HA) is a natural polysaccharide and a major component of the extracellular matrix and synovial fluids of the body. It binds to various cancer cells that over-express CD44, an HA receptor.<sup>12,13</sup> HA was utilized as a targeting moiety of the HSA-Gem conjugates for resistant pancreatic cancer therapy while green fluorescent GQDs were used for bioimaging of cancer cells.

Bioimaging or visualization of living cells is very important for medical diagnostic purposes. Previous studies have shown the extensive use of many fluorescent agents for this purpose, on

the other hand photobleaching and high cost of these compounds opens a gateway to find their better substitutes. Quantum dots-nano-entities made of semiconductor materials (cadmium, zinc, selenium) are an attractive option to be explored as bio-illuminators for living cells. Although they possess stable fluorescence, toxicity of cadmium and other semiconductor material is a cause of concern that restrains their biological application.<sup>14,15</sup> Graphene quantum dots (GQDs) on the other hand provide a much better option for their application as bioimaging agents due to their excellent photoluminescent, conductive and biocompatible properties.<sup>16,17</sup> In this study, the potential of GQDs conjugated human serum albumin nanoparticles for bioimaging and targeted drug delivery was explored and to the best of our knowledge, this is the first report coupling both HA and GQDs for pancreatic cancer specific nanoformulation.

The main objective of this study was to synthesize graphene quantum dots and to conjugate them with HA functionalized HSA-NPs for preparing a novel and efficient nano-delivery vehicle for pancreatic cancer specific drug delivery and bioimaging. HSA (molecular weight 65 kDA) is a plenteous protein in human blood plasma with a blood concentration of about 50 mg ml<sup>-1</sup> and it comprises of 585 amino acids along with 17 disulfide bridges.<sup>18</sup> For the synthesis of albumin nanoparticles a well established desolvation method was adopted. Basic mechanism of the process includes condensation of albumin and its interaction with ethanol and glutaraldehyde. Prior to final synthesis, different parameters (pH, glutaraldehyde concentration, crosslinking time) were optimized to prepare an efficient nanoformulation. pH of the solution plays a very important role in size control of HSA nanoparticles during the process because of its effect on coagulation of HSA molecules. The isoelectric point (pI) of HSA is about 4.7 and at pH range near its isoelectric point, coagulation increases due to enhanced protein-protein interaction which in turn results into larger particle size. While at pH values much higher than the pI, electrostatic repulsive conditions prevent interactions between protein molecules and protein-solvent interaction decreases the coagulation and fine HSA nanoparticles may be formed.<sup>19</sup> After working with different pH ranging from pH=7 to 10, it was concluded from the experimental data that at pH 9, particles of smallest size (56-250 nm) were obtained.

HSA possesses 59 free amines but while crosslinking with glutaraldehyde, residual surface amine level shrinks significantly therefore before nanoparticles synthesis, HSA was conjugated with dimethyl maleic anhydride (DMMA) to create amine-protected HSA as reported

elsewhere.<sup>20,21</sup> DMMA was detached from the surface amines via hydrolysis after synthesizing HSA-NPs. SEM images revealed the spherical morphology of HSA nanoparticles (Fig. 1) with mean particle diameter of approximately 150 nm (ranging from 56-250nm) and good dispersion. DLS histogram presents the size distribution of nanoparticles Fig. S1 (supplementary information). Nanospheres exhibit chemotherapeutic advantages of biodegradability and enhanced permeability and retention effect (EPR) for cancer therapy. Thus, these are the most applied form of drug delivery vector. Earlier studies have also shown that phagocytosis of tumor cells depends on size of nanoparticles and nanoparticles with 100-200 nm diameters exhibit preferential accumulation on tumor cells than healthy cells.<sup>22,23</sup> To confirm the functionalization of HA on HSA-NPs FT-IR spectroscopy was performed. As indicated in Fig. 2(i), apart from the characteristic peak of HA at  $3322\text{ cm}^{-1}$  due to O-H stretching, a peak corresponding to amide bond (CO-NH) at  $\sim 1680\text{ cm}^{-1}$  in the spectrum of HA-HSA confirms the modification of HSA-NPs with HA. Thermo Gravimetric analysis (TGA) revealed three step decomposition patterns for HSA nanoparticles (Fig. 3(i)) where as HA modified HSA exhibited an additional decomposition step as shown in Fig. 3 (ii). Specifically, for HA modification  $\sim 36.24\%$  weight loss occurred indicating a successful functionalization of HA on albumin nanoparticles.

Graphene quantum dots due to their photoluminescence and biocompatibility have attracted a lot of interest in their bioimaging applications as compared to their semiconductor counter parts. The two prime approaches for synthesizing GQDs can be classified as bottom-up and top down methods and various procedures have been reported based on these techniques for synthesis of GQDs.<sup>24-26</sup> In bottom up approach, quantum dots are synthesized from a carbon precursor containing conjugated carbon atoms where as top down methods involve cutting large graphene sheets. Although bottom up approach provides a precise control over size and morphology, the synthesis procedure is quite tedious and complicated. With regard to this, top down approaches are a better alternative with their simple methodology and mass production. GQDs were prepared via hydrothermal reduction of Graphene oxide (GO) with Lawsone and were further characterized for their optical properties. Hydrothermal approach of synthesis was adopted because of its simplicity, versatility and scalability. This is the first report demonstrating the synthesis of GQDs with Lawsone as a reducing agent. The synthesized particles exhibited excellent green fluorescence. Apart from the characteristic peak at 230 nm due to  $\pi$ - $\pi^*$  transition

of C=C domains, UV-Vis spectrum of GQDs also showed an absorption peak at 340 nm (Fig. S2). The peak at 340 nm represents the uniform  $sp^2$  clusters in GQDs.<sup>25</sup> An excitation dependent PL spectra was obtained from GQDs and two peaks at 430 nm and 540 nm were observed with 340 nm excitation whereas for 360-480 nm excitation, PL spectra was dominated by only one peak at 540 nm, responsible for green fluorescence of GQDs (Fig. 4). Zhu et. al. have also reported similar observations, expected to arise because of quantum size effects and surface defects due to variations in synthesis procedures.<sup>24</sup> Quantum yield of GQDs was ~14% and calculated as per the method described by Zhu et. al. at 360 nm excitation wavelength using 9,10-Bis (phenylethynyl) anthracene in cyclohexane (QY=1) as reference compound.<sup>24</sup> Fig. 5 shows TEM image of GQDs with an average diameter of ~5 nm while the supplementary fig. S3 represents the XRD patterns of samples before and after the hydrothermal reduction. The GO exhibited a sharp peak at  $11.5^\circ$ , which completely disappeared in reduced graphene sheets and a characteristic peak at  $26.6^\circ$  represents the reduction of GO to quantum dots. The FTIR spectrum of GQDs revealed the presence of C=O, O-H, epoxy/ether groups, which makes them water soluble. After conjugation of GQDs with HSA, apart from the characteristic peaks, a peak at  $1670\text{ cm}^{-1}$  which corresponds to amide bond (CO-NH) formation between the carboxy groups of GQDs and amino groups of HSA-NPs was observed (Fig. 2 (ii)). Zeta potential of blank HSA nanoparticles, HA-HSA and HSA-HA-GQDs was determined via dynamic light scattering (DLS) and found to be -27.78, -31.45 and -33.21 mV respectively. HA is negatively charged at physiological pH as indicated from the zeta potential analysis. The high surface charge indicates effective water suspension and is advantageous for storage and administration of nanoparticles. As previously reported, anionic nanocarriers are more preferred for targeted drug delivery than their cationic counterparts due to nonspecific binding of cationic vehicles to different cells after systemic administration. Moreover electrostatic repulsion among negatively charged nanospheres also prevents their aggregation to evade inactivity<sup>27-29</sup>. Considering these facts, it can be concluded that our graphene quantum dots conjugated system has the potential to be developed as an efficient drug delivery tool. UV-Vis analysis revealed that approximately 91% drug was encapsulated within the albumin nanoparticles (Fig. S4). Summarized details of size and other physiochemical properties of HSA-NPs and quantum dots are shown in Table S1.

HSA also exhibits excellent ligand binding capacity, stability in pH variations, noncovalent reversible binding properties and biocompatibility that makes it an ideal vector for transport and release of drugs to the cell surface. It consists of three homologous domains each comprises of two helical sub-domains with stable binding sites responsible for high affinity binding of various drugs at different therapeutic concentrations.<sup>30, 31</sup> HA functionalized Gem-HSA nanoformulation is more advantageous over other systems because of its specific targeting towards pancreatic cancer, sustained release of GEM and low toxicity to healthy cells. In our analysis, for gemcitabine loading, we amalgamated both the techniques (direct drug loading and physical adsorption at the surface of nanoparticles) to prepare nanoformulation with better encapsulation efficiency and release profile. Both the methods possess their own benefits and shortcomings i.e. direct loading suffers from the disadvantage of low encapsulation and loading efficiency in comparison to physical adsorption, but exhibits better sustain release properties than the latter one. The *in vitro* release profile of gemcitabine showed about 18 hrs sustained release at 37 °C in PBS (Fig. 6) and keeping in mind the high water solubility and short half life of gemcitabine due to its rapid metabolism, our HA functionalized nanoformulation is rather an improvement for pancreatic cancer specific drug delivery. A biphasic release pattern was obtained for gemcitabine with initial burst release followed by a slow release pattern up to ~18-20 hrs, the mechanism of which can be explained by drug leaching or detachment in first phase of fast release due to physically adsorbed drug on the surface of nanoparticles while first order diffusion controlled behavior was responsible for slow release of the drug.

Panc-1 cell lines are rich in CD-44, a receptor for Hyaluronic acid and responsible for chemotherapy resistant pancreatic cancer cells. To predict the cellular uptake of HSA-NPs and HA functionalized NPs, GQDs were tagged with the nanoparticles. A strong green fluorescence was observed inside the cells resulting from the efficient uptake of HA-HSA-NPs by Panc-1 cancer cells as shown in Fig. 7 (iii). On the other hand, unfunctionalized HSA-NPs exhibited weak fluorescence signal, indicating that a lesser amount of nanoparticles in comparison to HA-HSA-NPs are internalized into the cancer cells due to absence of the target moiety for CD-44 positive Panc-1 cells as exhibited in Fig. 7 (ii). It is clear evidence that HA-HSA-NPs can efficiently target CD-44 over expressing pancreatic cells via HA mediated endocytosis pathway.

After confirming the cellular uptake of nanoparticles, the anti-cancerous efficacy of nanoformulations was analyzed *in-vitro* via MTT assay. Panc-1 cells were incubated with HSA-Gem, HSA-HA-Gem and free gem. As shown in Fig. S5, HA-HSA-Gem formulation was the most effective one due its targeted internalization in CD-44 expressing PANC-1 cells. MTT data also revealed that Albumin and HA-HSA nanoparticles were quiet biocompatible and showed almost no toxicity to panc-1 cells with excellent cell viability 91-89 % respectively at different concentrations (5-20  $\mu\text{g/ml}$ ). Moreover the prepared GQDs were also biocompatible even at high concentrations (350-400  $\mu\text{g/ml}$ ). It can be concluded that our hyaluronic acid modified HSA-NPs has a theranostic potential to be an efficient nano-vector for treatment of pancreatic cancer, the deadliest in all cancers. Apart from improvising our system for prolonged release we are further focusing on *in-vivo* experimentations to check the proficiency of this formulation so that it can be developed like “Abraxane” to cure drug resistant pancreatic cancer.

### Conclusion

Hyaluronic acid and graphene quantum dots functionalized HSA nanoparticles were prepared and applied for bioimaging and targeted delivery of gemcitabine to pancreatic cancer. Due to the rapid metabolism and short half life of gemcitabine its efficacy gets reduced when administered in free form but with our nanoformulation we not only attained sustained release but also got notable effect on bioavailability of gem to cancer cells *in vitro* as exhibited by MTT assay. Presence of HA as targeting moiety on HSA-NPs is the essence of better efficiency of gem on resistant pancreatic cancer cells while GQDs exhibited excellent bioimaging potential. Experiments are being carried out to further improve this system for *in vivo* analysis.

### Acknowledgement

This work was supported by The Department of Science & Technology, Government of India. Author is grateful to Dr. Satish B. Ogale, Chief Scientist, National Chemical Laboratory for providing necessary guidance and help during the synthesis process of nanomaterials.

### Notes & References

<sup>a</sup> Combichem Bioresource Centre, National Chemical Laboratory, Pune India.

<sup>b</sup> Department of Chemistry, Garware College, Pune India

<sup>c</sup> Department of Microbiology, Fergusson College, Pune, India.

<sup>#</sup> Equal first author

1. S. Yachida and C. A. Iacobuzio-Donahue, *Arch. Pathol. Lab. Med.*, 2009, **133**, 413-422.

2. A. L. Papa, S. Basu, P. Sengupta, D. Banerjee, S. Sengupta and R. H. Papa, *BMC Cancer*, 2012, **12**, 419.
3. G. Y. Lee, W. P. Q. L. Wang, Y. Q. A Wang, C. A. Staley, M. Satpathy, S. Nie, H. Mao and L. Yang, *ACS Nano*, 2013, **7**, 2078-2089.
4. Kalluri and R. Zeisberg, *Nat. Rev. Cancer*, 2006, **6**, 392-401.
5. R. F. Hwang, T. Moore, Arumugam, T. Ramachandran, V. Amos, K. D. Rivera, A. Ji, D. B. Evans and C.D. Logsdon, *Cancer Res.*, 2008, **68**, 918-926.
6. J. Nicolas, S. Mura, D. Brambilla, N. Mackiewicz and P. Couvreur, *Chem. Soc. Rev.*, 2013, **42**, 1147-1235.
7. M. Shi, J. Lu and M. S. Shoichet, *J. Mater. Chem.*, 2009, **19**, 5485-5498.
8. B. Asadishad, M. Vossoughi and I. Alemzadeh, *Ind. Eng. Chem. Res.*, 2010, **49**, 1958-1963.
9. M. Foote, *Biotechnol. Annu. Rev.*, 2007, **13**, 345-357.
10. R. L. Kleynberg, A. A. Sofi and R. T. Chaudhary, *A. M. J. Ther.*, 2010, **18**, e261-e263.
11. S. P. Hong, J. Wen, S. Bang, S. Park and S. Y. Song, *In. J. Cancer*, 2009, **125**, 2323-2331.
12. V. M. Platt and F. C. Szoka, *Mol. Pharmaceutics*, 2008, **5**, 474-486.
13. S. S. Khurana, T. E. Riehl, B. D. Moore, M. Fassan, M. Ruge, J. Romero-Gallo, J. Noto Jr. R. M. Peek, W. F. Stenson, and J. C. Mills, *J. Biol. Chem.*, 2013, **288**, 16085-16097.
14. N. Chen, Y. He, Y. Su, X. Li, Q. Huang, H. Wang, X. Zhang, R. Tai and C. Fan, *Biomaterials* 2012, **33**, 1238-1244.
15. M.C. Mancini, B.A. Kairdolf, A. M. Smith and S. Nie, *J. Am. Chem. Soc.* 2010, **130**, 10836-10837.
16. A. A. Nahain, J. E. Lee, I. I. Haeshin, L.K. D. Lee, J. Hoon Jeong, and S. Y. Park *Mol Pharmaceutics* 2013, **10**, 3736-3744.
17. J. Shen, Y. Zhu, X. Yang and C. Li, *Chem. Commun.*, 2012, **48**, 3686-3699.
18. K. Langer, S. Balthasar, V. Vogel, N. Dinauer, H. V. Briesen and D. Schubert, *Int. J. Pharm.*, 2003, **257**, 169-180.

19. S. Ko and S. Gunasekaran, *J. Microencapsul.*, 2006, **23**, 887-898.
20. B. Sungho, M. Kyungwan, T. H. Kim, E. S. Lee, K. T. Oh, E.S. Park, K. C. Lee and Y. S. Youn , *Biomaterials* , 2012, **33** ,1536-1546.
21. Y.S. Youn, S.Y. Lee, J.E. Jeon, H.G. Shin and K.C. Lee, *Biochem Pharmacol*, 2007, **73**, 84-93.
22. S. K. Hobbs, W. L. Monsky, F. Yuan, W. G. Roberts, L. Griffith and V. P. Torchilin, *Proc Natl Acad Sci*, 1998, **95**, 4607–4612.
23. Z. Shena, Y. Li, K. Kohamab, B. Oneilla and J. Bi, *Pharmacol. Res.*, 2011, **63**, 51–58.
24. S. Zhu, J. Zhang, C. Qiao, S. Tang, Y. Li, W. Yuan, B. Li, L. Tian, F. Liu, R. Hu, H. Gao, H. Wei, H. Zhang, H. Sunb and B. Yang *Chem. Commun.*, 2011, **47**, 6858–6860.
25. D. Pan, J. Zhang, Z. Li and M. Wu, *Adv. Mater.*, 2010, **22**, 734-738.
26. S. Wu, F. Tian, W. Wang, J. Chen, M. Wu and J. X. Jhao, *J Mat Chem C*, 2013, 1, 4676-4684.
27. S. K. Hobbs, W. L. Monsky, F. Yuan, W. G. Roberts, L. Griffith and V. P. Torchilin, *Proc Natl Acad Sci*, 1998, **95**, 4607–4612.
28. Z. Shena, Y. Li, K. Kohamab, B. Oneilla and J. Bi, *Pharmacol. Res.*, 2011, **63**, 51–58.
29. M. Chacon, J. Molpeceres, L. Berges, M. Guzman and M.R. Aberturas , *Eur. J. Pharm. Sci.*, 1999, **8**, 99-107.
30. J. Gang, S. B. Park, W. Hyung , E. H. Choi ,J. Wen and H. S. Kim, *J. Drug Target*, 2007,**15**, 445-453.
31. M. Celano, M. G. Calvagno , S. Bulotta ,D. Paolino , F. Arturi and D. Rotiroti , *BMC Cancer*, 2004, **4**, 63-67.

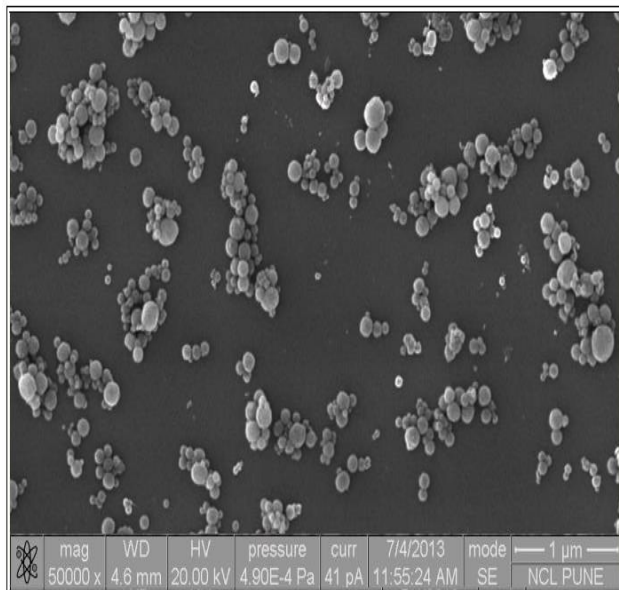


**Figure 1:** SEM image of HSA nanoparticles.

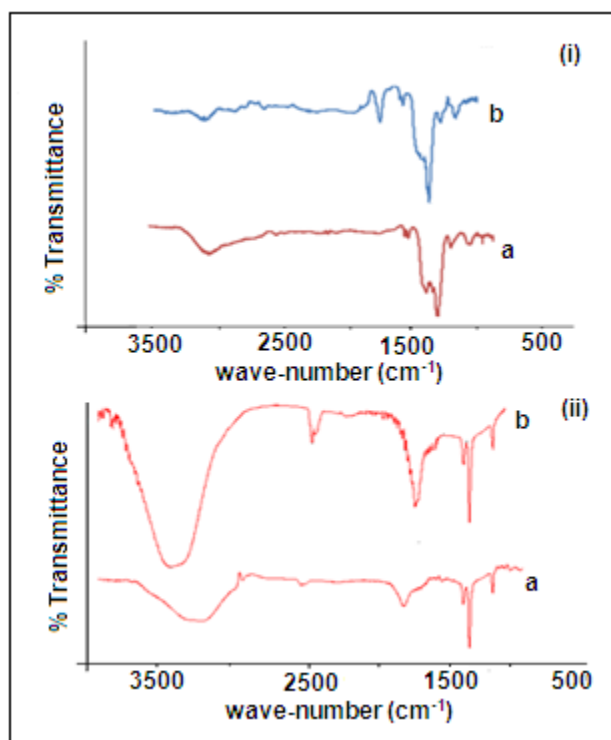


**Figure 2:** (i) FTIR spectra of (a) Hyaluronic acid, (b) HSA-Hyaluronic acid functionalized nanoparticles; (ii) FTIR of (a) GQDs; (b) HSA-GQD functionalized nanoparticles.

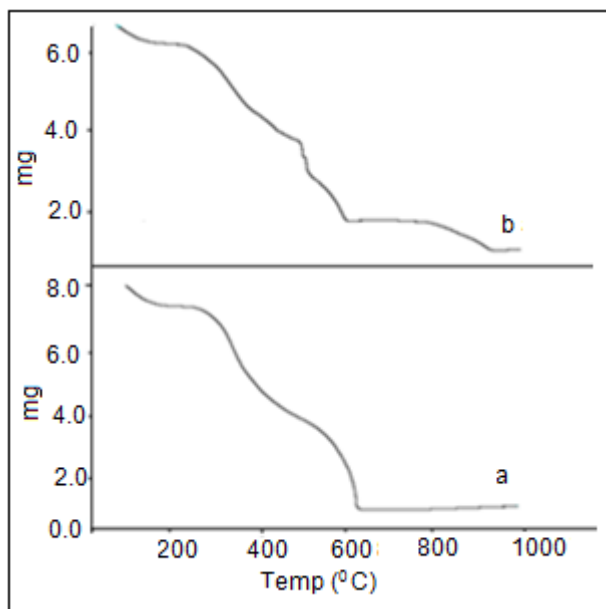


**Figure 3:** TGA curve of (a) Albumin nanoparticles, (b) Hyaluronic acid functionalized albumin nanoparticles (Ramp rate:  $10^{\circ}\text{C}/\text{min}$  in nitrogen environment).

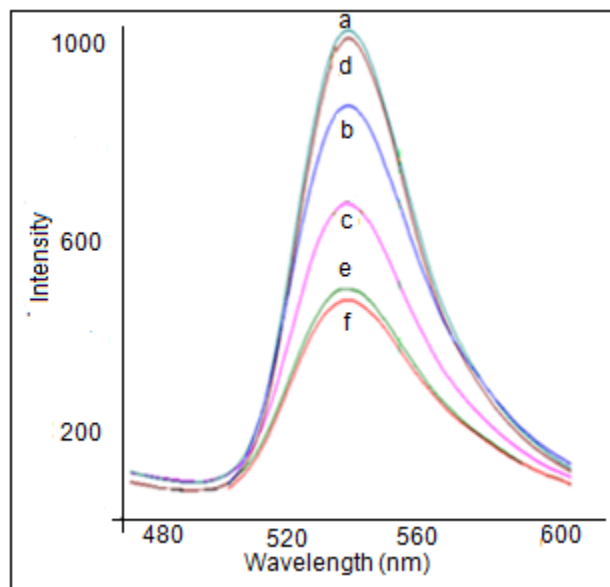


**Figure 4:** PL spectrum of aqueous solution of graphene quantum dots at excitation wavelength of 360-480 nm (a) 360 nm, (b) 400 nm, (c) 420 nm, (d) 440 nm, (e) 460 nm, (f) 480 nm. (Experiments were performed at room temperature ( $\sim 25^{\circ}\text{C}$ )).

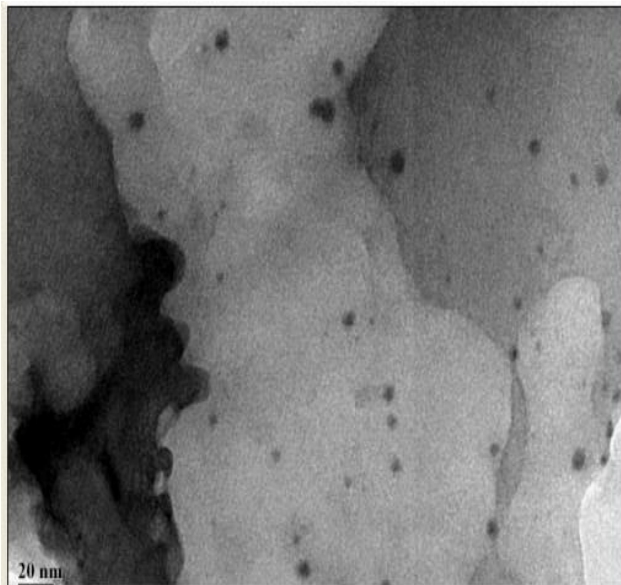


**Figure 5:** TEM of graphene quantum dots (average particles size ~5 nm).

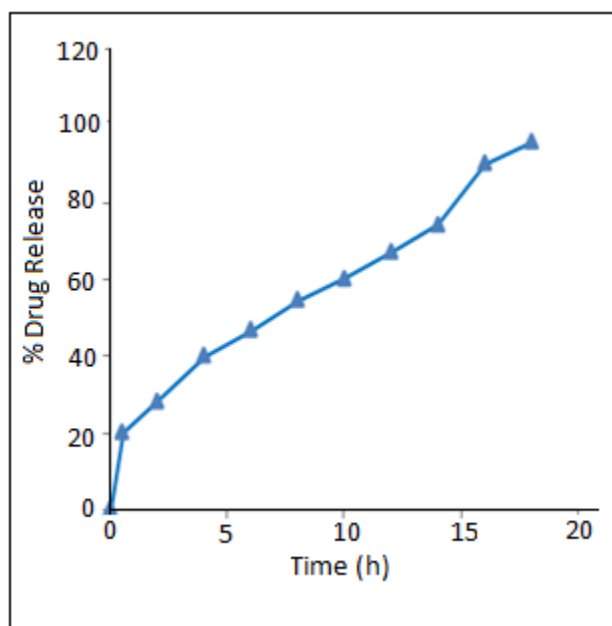


**Figure 6:** *in-vitro* release profile of gemcitabine from HSA nanoparticles in PBS (pH=7.0) at 37<sup>0</sup> C.

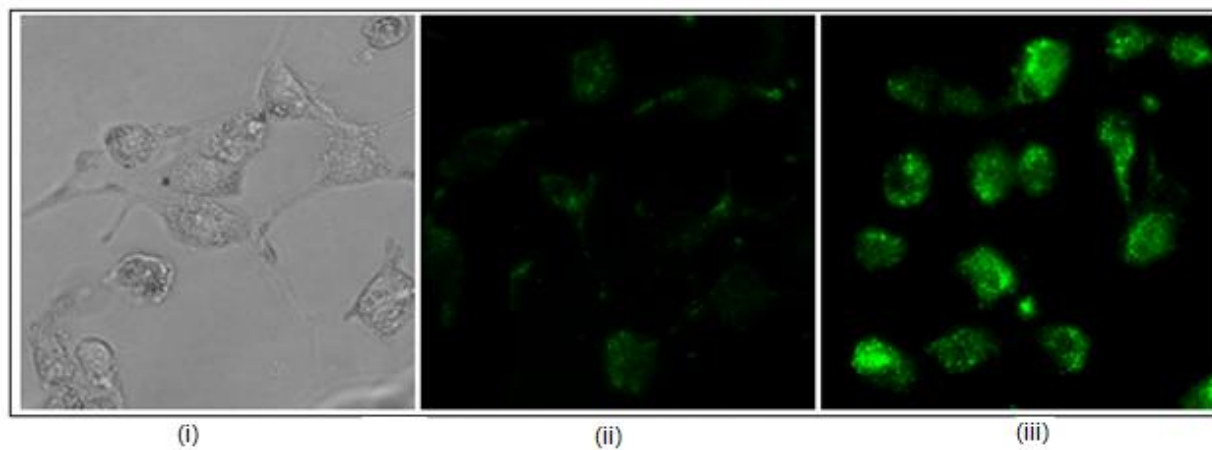


**Figure 7:** Fluorescence imaging of Panc-1 cells after 24 hrs incubation in presence of GQDs conjugated HSA nanoparticles in DMEM media with 10 % FBS in CO<sub>2</sub> incubator at 37 °C; (i) Cells without staining (control), (ii) HSA nanoparticles with GQDs only, (iii) HSA NPs functionalized with HA and GQDs.